

## A Comparison of Neural Network and Multiple Regression Transmission Line Icing Models

P. MCCOMBER<sup>1</sup>, J. DE LAFONTAINE<sup>1</sup>, J.A. DRUEZ<sup>2</sup>,  
J. LAFLAMME<sup>3</sup>, AND A. PARADIS<sup>1</sup>

### ABSTRACT

An increasing number of high voltage transmission lines are exposed to atmospheric icing in remote northern regions. Instrumentation able to operate unattended in this remote environment is increasingly being designed in conjunction with appropriate icing models to estimate transmission line icing. Hydro-Québec has implemented such a system (SYGIVRE) relying on the Mt. Bélair icing site to collect icing data required to improve the system. Mt. Bélair offers a high voltage transmission line instrumented with load cells besides icing instrumentation. Measurements of average temperature, wind speed and direction, precipitation rate and the number of icing rate meter (IRM) signals are also recorded on the site with one hour periods. Icing data have been collected between 1994 and 1998 and constitute the data base on which a model can be developed to be used at other sites eventually.

This paper investigates two techniques, multiple-variable linear regression and the neural network, to develop icing models and estimate a cable icing rate from the same set of hourly measurements. Results show that the neural network is a slightly more accurate model even though the difference in accuracy of the two models is small. However, the design of an appropriate neural network which has a more complicated structure usually requires more time initially in comparison with the multiple regression approach which has an advantage in its simplicity.

**Keywords :** Atmospheric icing, neural networks, multiple linear regression, transmission line icing, ice accretion

### 1. INTRODUCTION

Atmospheric icing of structures is a relatively rare meteorological phenomenon often occurring in remote northern regions. Presently, it remains important to develop both appropriate instrumentation and reliable atmospheric icing models to be able to estimate icing loads as accurately as possible before serious damage can occur. Such models have to be developed to make optimal use of the scarce icing data already available.

Many different icing models have been developed to compute cable icing loads. These can be divided in two main groups. The first kind of model is based on physical or mathematical equations, attempting to describe the physical process of an ice accretion (Poots 1996). This approach has the advantage of being independent of the icing site, but usually rely on variables not easily measured, e.g. liquid water content or droplet sizes.

Due to the difficulty in obtaining data and also due to the inaccuracy of this data a second kind of models, empirical models, have also been adopted to obtain icing load estimate closer to measured values. The simplest model of this kind can be obtained by using multi-variable linear regression to relate instrumentation readings to measured cable load (McComber et al. 1995). Recently, neural networks offer a new approach within the empirical model family for modeling transmission line icing (Ohta et al. 1996; Wakamatsu et al. 1993). It uses directly measured data to teach or train the model, i.e. optimize its parameters, to give the right answer when the appropriate data is fed in. Neural networks are emerging as a legitimate means of modeling such a complex phenomenon as ice accretion. Furthermore, in the case of prediction of transmission line icing,

<sup>1</sup> Département de génie mécanique, École de technologie supérieure, 1100, rue Notre-Dame Ouest, Montréal, Québec, H3C 1K3 Canada

<sup>2</sup> Département des Sciences appliquées, Université du Québec à Chicoutimi, 555 Boul. Université, Chicoutimi, Québec, G7H 2B1 Canada

<sup>3</sup> Hydro-Québec, 800 Maisonneuve est, Montréal, Québec, H2L 4M8 Canada

neural networks associated with appropriate instrumentation provide a means of synthesizing a virtual instrument to measure the icing load directly. The data recorded by the various instruments can then be interpreted as an icing rate on the conductors.

Since both techniques have advantages and disadvantages, this paper compares their respective results using the same icing input data.

## 2. TYPES OF ATMOSPHERIC ICING AFFECTING STRUCTURES

Three basic kinds of ice are formed by accretion in the atmosphere: glaze, hard rime and soft rime. Glaze is transparent and it has a density with respect to water of approximately 0.9 (the density of pure ice is 0.917). Hard rime is white and sometimes opaque, depending on the quantity of air trapped inside the ice. Its density varies from 0.6 to 0.9. Soft rime is white and opaque. It is feathery or granular in appearance with a density less than 0.6. The density will increase with increasing drop size, temperature, wind speed and liquid water content.

Cloud or fog droplets have diameters smaller than 200  $\mu\text{m}$ . Cloud droplet sizes measured experimentally indicate that low level clouds, which can affect a structure on a mountain summit, have droplet sizes in the 1-45  $\mu\text{m}$  range. Consequently, exposure to super-cooled clouds or fog will usually result in soft rime. Freezing precipitations have droplets larger than 200  $\mu\text{m}$ . The higher liquid water content associated with the precipitations can produce hard rime or even clear ice. The boundary between in-cloud and freezing precipitation icing is difficult to establish on a mountain icing site where clouds and precipitations are often mixed and where the icing obtained varies in density, covering the range from soft to hard rime.

## 3. TRANSMISSION LINE ICING DATA

The icing data which is used as the data base for the comparison of the two transmission line icing models was obtained at the Mt Bélair icing site. This test site is located at an altitude of 490 m, 25 km northwest of Québec City and 9 km north of the Québec Airport, in a corridor formed by the Laurentian Valley. The main winds generally travel northeast (along the axis of the St. Lawrence River) and experience uplift when they pass over Mt. Bélair. On Mt. Bélair summit in-cloud icing and

freezing rain are relatively frequent from November through April. This test site provides measurements of several meteorological parameters, and records mainly wind and ice loads directly on a live 315-kV transmission line. As depicted in Fig.1, a load cell is installed on the tower which supports the 315-kV line. The site is equipped with two heated anemometers located on the 315-kV line at 12 m and 10 m above the ground and about 15 m away from the 315-kV line.

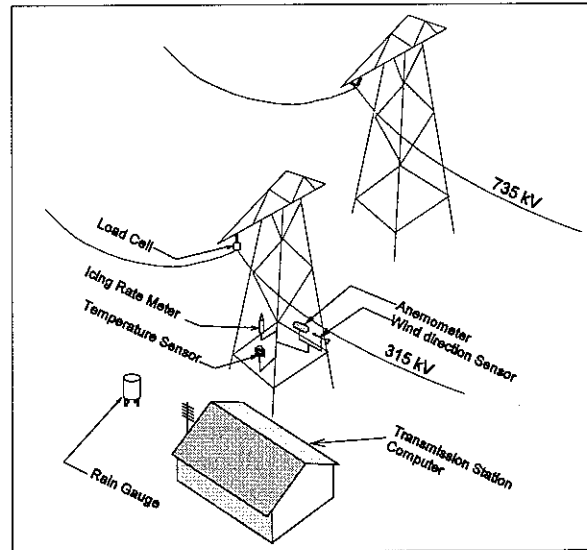


Figure 1. Schematic description of the Mt. Bélair test site.

Data have been continuously recorded starting in November of 1994. However, initially some meteorological parameters were not available due to instrumentation failures. For instance, the precipitation gauge did not work when first installed, the anemometers were out of order part of the time during some icing events. These anemometer problems were probably related to icing from freezing precipitation. Hydro-Québec's site experienced 20 icing events caused by freezing rain or in-cloud icing between the fall of 1994 and the spring of 1997. All variables are dynamic and random so that averages are taken and hourly recorded. The recorded data were broken down in one hour periods to form the data base necessary for the models. The hourly values for each variable for all of the events give a total number of 526 points. Three quarters (75%) of this data (393) were used in developing the model and the remaining quarter (25% or 133) were used to validate them.

The neural network and the linear regression models make use of four instrument signals as input: temperature, wind velocity normal to the power line, precipitation and IRM signals.

After testing a simpler network with four inputs: temperature, precipitation rate, IRM (icing rate meter) signals and normal wind speed, a ten (10) input model was developed to take into account the dynamic aspect of this process. The same four parameters are used but values at previous time steps are simultaneously taken as inputs. Temperatures, IRM signals and precipitation rate are used at time steps  $t$ ,  $t-1$  and  $t-2$  giving nine of the inputs while only the most recent wind speed is included. Wind speed is treated differently because additional inputs for this variable did not improve the results. A comparison between the simpler four input network and the ten input network has shown a significantly better performance for the latter (Mccomber et al. 1998). The ten inputs, described in Table 1, are therefore retained and used in the comparison with multiple linear regression that follows.

**Table I. Description of the inputs**

<i>Input</i>	<i>Symbol</i>	<i>Description</i>
$i_1$	$IRM_t$	<i>IRM signals at t</i>
$i_2$	$IRM_{t-1}$	<i>IRM signals at t-1</i>
$i_3$	$IRM_{t-2}$	<i>IRM signals at t-2</i>
$i_4$	$P_t$	<i>Precipitation at t</i>
$i_5$	$P_{t-1}$	<i>Precipitation at t-1</i>
$i_6$	$P_{t-2}$	<i>Precipitation at t-2</i>
$i_7$	$T_t$	<i>Temperature at t</i>
$i_8$	$T_{t-1}$	<i>Temperature at t-1</i>
$i_9$	$T_{t-2}$	<i>Temperature at t-2</i>
$i_{10}$	$V_t$	<i>Wind speed at t</i>

The input data are normalized on a 0-1 scale by dividing each positive variable by its maximum range. For temperatures, positive values are first obtained by the addition of an arbitrary constant. The output or target is the hourly increasing in ice load,  $\delta m_i$  (kg/m.h). It is compared with the load measured by a load cell on one of the six conductors on the 315 kV line. The hourly data are used to find the icing rate,  $\delta m_i$  (kg/m.h) and the following expression is then used to find the resulting ice mass as a function of time.

$$m_{i+1} = m_i + \delta m_i \delta t \quad (1)$$

The above equation corresponds to a first order numerical integration scheme, but the additional inputs at previous time steps associated with their optimized coefficients make Eq. (1) equivalent to a higher order integration method.

#### 4. THE NEURAL NETWORK MODEL

##### Neural Networks

Biologically inspired neural networks are finding increased applications in modeling of complex dynamical systems. The book by Amat and Yahiaoui (1995) provides one of the many available introductions to this field.

The basic elements of a neural network are schematically shown in Fig. 2, which also describes the network structure used for the icing model. Several inputs are connected to the neurons (nodes or processing elements that form a layer). In general there can be more than one hidden layers, followed by the output layer. The number of connections is higher than the total number of nodes. Both numbers are chosen based on the particular application and can be arbitrarily large for complex tasks. Simply put the multi-task job of each neurons is to evaluate each of the input signals, to calculate the weighted sum of the combined inputs, to compare that total to some threshold level, and finally to generate the output. The various weights are the adaptive coefficients which vary as the network learns to perform its assigned tasks using the training data and making some inputs are more important than others. The threshold or activation function is generally nonlinear. The most common one, used below, is the continuous logsigmoid, or S-shaped, curve which approaches a minimum (0 or -1) and a maximum (+1) value at the asymptotes. If the sum of the weighted inputs is larger than the threshold value, the neuron generates a signal (+1); otherwise a zero signal is fired. The neural networks described in Fig. 2 operates in feedback mode. This terminology refers to the direction of information through the network. The self-learning network updates its various parameters by comparing its input to a desired output, thus requiring feedback information relating to the effect of its control.

Complex systems for which dynamical equations may not be known or may be too difficult to solve, can be modeled using neural nets. One of their advantages is their ability to approximate to any degree of accuracy any measurable function: they are so-called universal "approximators" (Hornick et al. 1989; Chen

and Chen 1993). However, mathematical proofs on the existence of an accurate representation do not necessarily tell the designer which structure is the right one. Then comes the problem of convergence (Nordgren and Meckl 1993) of the neural networks representation (has its parameters converged to the real characteristics of the dynamical system?), and the problems of asymptotic stability (is the neural network able to bring the error to zero?)

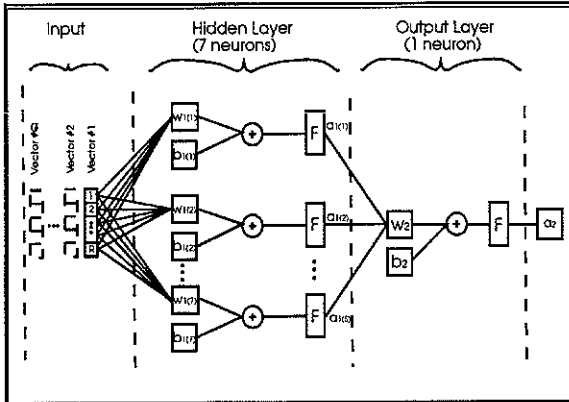


Figure 2. Example of a neural network

Some of the design characteristics of neural networks as applied to an icing model were addressed in a previous paper (McComber et al. 1998) the final choice of the structure of the network is illustrated in Fig. 2. The neural network described in the present paper is the best one developed to date with the available data.

### Neural network learning rule

The back-propagation learning rule is used to train the network. It minimizes the sum of squared errors (*SSE*) of the network by adjusting the weights and biases using a non-linear optimization technique. The delta vectors (derivatives of error) are calculated for the output layer, and back-propagated through the network to obtain the delta vector for the hidden layer.

Weights and biases are adjusted, based on the gradient descent technique, by moving them in the opposite direction to the error gradient. A fast technique of optimization using an approximation of Newton's method called the Levenberg-Marquardt's method was used for the present network.

The modification of the weights  $W_i$  at each step or epoch of this optimization technique is found by the following:

$$\Delta W = (J^T J + \mu I)^{-1} J^T e \quad (2)$$

where  $J$  is the Jacobian matrix of the error derivatives with respect to weights,  $\mu$  is a scalar and  $e$  stands for the error vector. If  $\mu$  is very large, then Eq. (2) approximates gradient descent and if it is small Eq. (2) becomes the Gauss-Newton method,  $\mu$  is adjusted during the processing.

### Definition of the minimized network error

The definition of the sum of squared errors (*SSE*) is the following:

in this equation  $Q$  is the number of test cases (elements of each input vector = 393),  $t$  is the

$$SSE = \sum_{k=1}^Q e(k)^2 = \sum_{k=1}^Q (t(k) - a(k))^2 \quad (3)$$

target value and  $a$  the corresponding output of the neural system.

### Neural network structure

The structure with one hidden layer of seven (7) neurons, shown in Fig. 2, was obtained by trial and error using the training and test data.

The number of neurons in the hidden layer can be increased further. The error on the training data would decrease but at the same time the error on the test data increases. The seven (7) neurons of the hidden layer is a compromise to obtain a reasonable error on the test data. The comparison between the training and test data will be presented in the results below.

Table 2 gives the weights and biases of the best neural network obtained.  $W1$  and  $B1$  refer to the weights and biases of the hidden layer.  $W2$  and  $B2$  refer to the output layer.

## 5. MULTIPLE-VARIABLE LINEAR REGRESSION MODEL

Linear regression uses a linear equation to relate the icing rate to the ten (10) input parameters, listed in Table 1.

$$\delta m_i = \beta_0 + \beta_1 i_1 + \beta_2 i_2 + \beta_3 i_3 + \dots \quad (4)$$

where  $i_i$  are the inputs and  $\beta_i$  are the linear coefficients to be calculated. Each one hour period icing is considered as a point of a  $n$ -point data set. This technique was previously used by McComber et al. (1993) to determine the icing rate from the number of IRM signals.

**Table 2. Weights and Biases of the neural networks**

$W_i$	$IRM_t$	$IRM_{t-1}$	$IRM_{t-2}$	$P_t$	$P_{t-1}$	$P_{t-2}$	$T_t$	$T_{t-1}$	$T_{t-2}$	$V_t$
$n_1$	1.8275	-14.65	-14.81	6.9162	-2.566	2.4462	0.1219	-1.738	-1.815	6.227
$n_2$	4.8717	-1.324	-0.244	1.9555	-4.022	-2.278	4.2054	0.5432	1.9203	0.101
$n_3$	-1.48	2.7582	1.6703	-13.14	8.5755	0.5386	-27.67	8.5621	14.914	1.821
$n_4$	40.079	29.939	26.817	33.838	-33.27	-22.95	14.718	-1.508	-9.37	8.527
$n_5$	-1.816	-5.451	-11.6	19.267	4.1279	1.3059	-3.257	0.08	0.2757	1.943
$n_6$	-8.475	-2.061	2.629	-1.272	0.2248	-14.34	-8.78	-2.002	-3.812	-6.86
$n_7$	-11.3	-5.439	-3.106	-2.326	-5.234	-0.874	5.4633	-0.694	-5.548	8.423

**Table 2 (continued)**

	$B_1$	$W_2$	$B_2$
$n_1$	-11.3257	-0.7284	0.496
$n_2$	12.5896	-2.4962	
$n_3$	4.6652	-3.2231	
$n_4$	-9.8602	1.201	
$n_5$	-3.229	-6.709	
$n_6$	-5.003	7.9183	
$n_7$	-2.5737	-8.4053	

The multiple regression coefficients minimizing the sum of squared errors SSE are given in Table 3.

**Table 3. Multiple-variable linear regression coefficients**

Coefficients	Value	Corresponding variable
$\beta_0$	0.011955	
$\beta_1$	0.006905	$IRM_t$
$\beta_2$	-0.002712	$IRM_{t-1}$
$\beta_3$	-0.003731	$IRM_{t-2}$
$\beta_4$	-0.000394	$P_t$
$\beta_5$	-0.0001	$P_{t-1}$
$\beta_6$	0.003173	$P_{t-2}$
$\beta_7$	-0.001385	$T_t$
$\beta_8$	0.005255	$T_{t-1}$
$\beta_9$	-0.000171	$T_{t-2}$
$\beta_{10}$	0.000788	$V_t$

The matrix equivalent of Eq. (4) for the  $n$  points is  $Y = X\beta$ , where  $Y$  is the column vector of the icing rates,  $\delta m_i$ , and  $X$  is a  $n \times 11$  matrix where a row corresponding to one of the  $n$  points is formed of 1 in the first column followed by 10 input variables  $[i_1 \ i_2 \dots \ i_{10}]$ . Then the vector of the eleven coefficient  $\beta$  is found by the solution of the linear matrix equation (Hines and Montgomery 1980):

$$X^T X \beta = X^T Y \quad (5)$$

The sum of squared errors SSE is found from:

$$SSE = Y^T X - \beta^T X^T Y \quad (6)$$

## 6. RESULTS OF THE COMPARISON

Results are presented in two parts. The first part is a comparison of the performance of the two models in predicting the icing rate on the complete set of test data. The second part of the comparison shows the application of the two models to the calculation of the total load for three (3) complete icing events.

### 6.1 Comparison of the model performance on the test data.

The data available to develop the two models were randomly divided in two groups: three quarters of the data (393) cases were used for the training. The main characteristics of the two models were established with these data by reducing to the maximum the error (SSE).

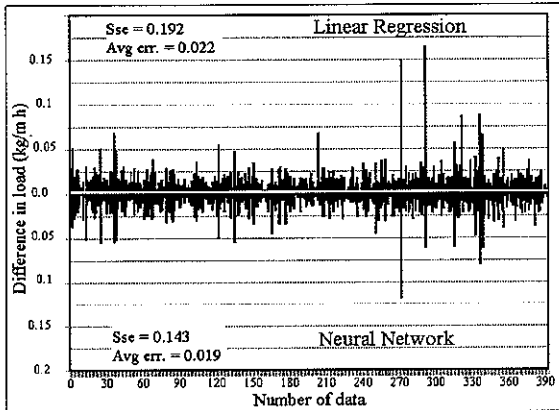


Figure 3 Comparison of the absolute value of the error in icing rate estimation for the training data

The resulting neural network model and multiple-variable regression were then used to compute the hourly icing rate (kg/m.h) and compared with the measured icing rate. The difference in icing rate is shown in Fig. 3 for each training case.

To facilitate the comparison, the absolute error is compared by putting above the axis the neural network results and below the axis the linear regression results. The remaining data (25% or 133 cases) were put aside in order to evaluate the resulting neural network with the new data (Fig. 4). The same basis for comparison was applied for these test cases.

Figures 3 and 4 show that the error is quite similar with both approaches, since the larger or smaller errors occur for the same hourly data. As would be expected, the sum of squared errors is

somewhat smaller for the training data shown in Fig. 3. However, whereas the neural networks is more accurate (a smaller SSE) on the training data the opposite is true for the test data. This is consistent

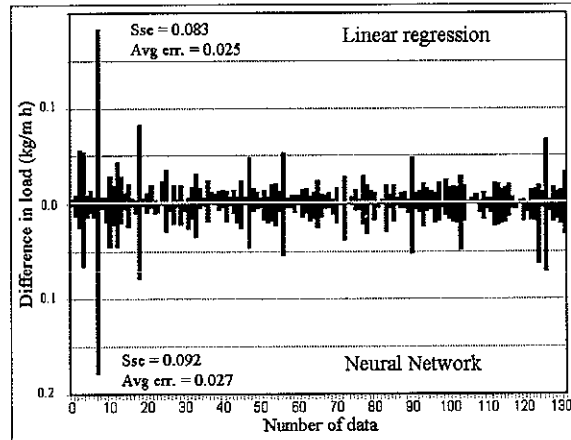


Figure 4. Comparison of the error in the icing rate estimation for the test data

with other tests done on the neural network in that increasing the accuracy of the training data (e.g. by increasing the number of neurons), decreases the accuracy on the test data.

The difference in estimated and measured loads displayed in Fig. 3 for the training data is approximately 0.025 kg/m.h for most of the test points. Only a small number of cases yield a larger difference. Usually, a larger error is obtained when the test data is out of the training range for some input variables. In these specific cases, the measured variables could be reexamined in order to determine possible causes of this larger sum of squared errors. The differences obtained in Fig. 4 on the test data are on the average slightly larger. However, test cases are a good indication that the two models will also be able to perform an icing rate estimation on new icing data with the same accuracy as long as the characteristics of the icing site, instrumentation and transmission line are relatively similar.

### 6.2 Model simulation on specific icing events

The two models are compared by making a simulation of three (3) complete icing events comparing with measurements recorded. The first two events chosen are the 19<sup>th</sup> January 1998 event shown in Fig. 5 and the 25<sup>th</sup> December 1997 shown in Fig. 6. The icing data used in these two cases were not part of the original set of data, so that it is a good indication of the performance of the models on new data. The final errors in Fig. 5 are -19.3% for the

neural network and -26.7% for the linear regression. For Figs 6 the corresponding numbers are -8.9% and 26.9%. Hence, in both cases the simulation done with the neural network is better.

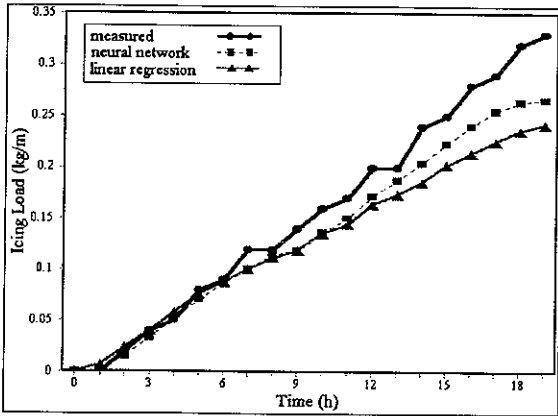


Figure 5. Comparison of the total ice load for the 19th January 1998 event

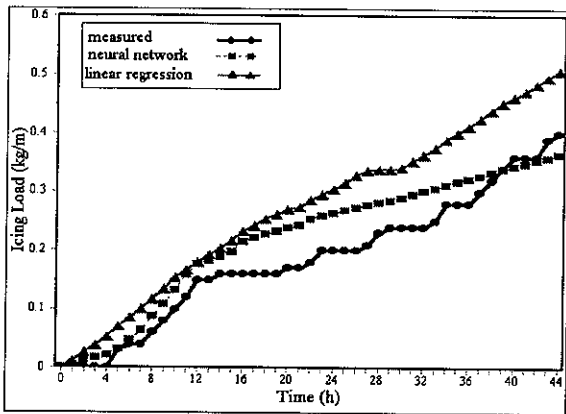


Figure 6. Comparison of the total ice load for the 25th December 1997 event

The third event, 7<sup>th</sup> December 1996 shown in Fig. 7 was chosen because of its duration and importance. In this case the errors on the end values are -33.4% for the neural network and -15.5% for the linear regression. Although the end value is better with the linear regression, a closer at Fig. 7 shows that the neural network is much better for the first 40 hours, but after that time, corresponding to the end of precipitation, both models underestimate the rate so that for the linear regression the smaller negative difference comes for a cancellation of error since it overestimated the rate in the first 40 hours.

Overall, the neural network is slightly better. For the first two cases, Fig. 5 and Fig. 6, the end values are better for the neural network model. For the third

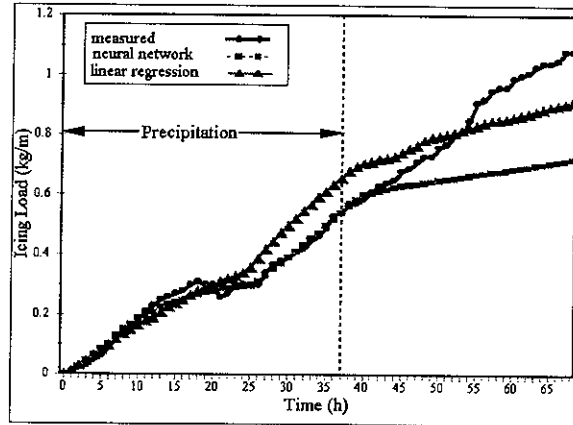


Figure 7. Comparison of the total ice load for the 7th December 1996 event

case (Fig. 7), the smaller negative error at the end of 69 h is a compensation for a larger positive error earlier at 40 h.

## 7. DISCUSSION

The linear regression coefficients give a good idea of the relative sensitivity of the different inputs (Table 3). Since the ten inputs were normalized, the magnitude of the coefficients reflects the sensitivity of the output to each input variable. Wind speed at time  $t$  has a smaller coefficient. For temperature and for the number of IRM signals, the coefficients,  $\beta$  at  $t$ , are larger than the ones at  $t-1$  and  $t-2$ . Precipitation is an exception with a smaller sensitivity for the time  $t$ . This particularity can be explained by the fact that precipitation corresponds to freezing rain whereas icing occurs also without precipitation for in-cloud icing. In-cloud icing is probably the source of a significant error of the models. In the two examples presented where measured icing loads continue to increase at a smaller rate towards the end of the event, a verification of the original data has confirmed that this behavior was associated with very small or no precipitation recorded.

The input data was initially randomly divided in two groups for training and testing of the models. This random selection prevents any bias in the input data. Also, since the number of points in the data base necessary for the network training increases both with the number of input variables and with the complexity of the approximated phenomenon, additional data provided by new icing events is always useful and will certainly improve the network performance.

With neural networks, multiple-variable regression or any other artificial intelligence techniques the

parameters are optimized for the data measured and the instrumentation. Since the usefulness of such a system lies in its use in as many different locations and condition settings as possible, it would be advantageous to standardize the instrumentation so that data collected on different icing sites could all be combined with the training data. Expert systems have the advantage of being well adapted to the data on which the training process is based. For example, if one of the instruments makes a systematic error in the parameter it measures the network will integrate this error and yield nevertheless an accurate icing rate. For example, the precipitation gauge might have such a systematic error in measuring precipitation rate at sub-freezing temperatures. The disadvantage of this characteristic is that a system optimized for a given data set is not automatically accurate on other sites not equipped with similar instrumentation.

Neural networks have the characteristic that, after reaching a certain level of accuracy, as they become more accurate on the training data they tend to become less accurate on the test or validation data. This characteristic probably applies to different icing sites. Making the model too accurate on the Mt. Bélair data might make it less accurate in other locations and for other instrumentation.

## 8. CONCLUSIONS

In this paper, a neural network technique was compared with a multiple-variable linear regression model for determining icing loads on transmission lines using the same icing data inputs collected on the icing site of Mt. Bélair. The models use four parameters as inputs: temperature, precipitation rate, number of IRM signals and normal wind speed. The data base is obtained from measurements from twenty in-cloud icing events during the 1994-1997 period and divided into one hour periods of icing to provide the experimental icing rate data base. The target data is the icing rate as measured icing on a 35 mm cable of a 315 kV transmission line.

Both models had ten (10) variables as inputs using measurements of temperature, precipitation rate and Icing Rate Meter (IRM) signals at previous time steps. This number of inputs was shown to be more accurate probably by taking into account the dynamic characteristics of the phenomenon.

The neural network with the best performance had only one hidden layer of seven neurons. One hidden layer of neurons was retained with an optimal

number of six neurons. The activation or output function of each neuron was a logsigmoid function.

Both models were optimized using the same set of input data by finding the minimum of the sum of the squared errors (SSE). The two types of models were compared both with the training and validation data. For the training data the neural network yielded a smaller sum of squared errors whereas for the test data the opposite was true. The comparison of total icing loads estimated for complete icing events gave a small advantage to the neural network model.

The parameters of each model were determined by optimization. The procedure for the linear multi variable regression model is straightforward and consists in the solution of a single matrix equation. However, the neural network model requires a non-linear optimization procedure. The solution is obtained by an iterative gradient method which is more complex since it requires initialization of its coefficients and does not always converge to the same optimal parameters.

Both methods have a common advantage of adapting to new data as they become available, the training can be made continuously. Neural networks offer the advantage of flexibility associated with its complex structure and non linear characteristics. But this is balanced by the difficulty in initializing the system and attaining convergence. Multiple-variable linear regression has the advantage of simplicity and can be used as a first approximation and as a benchmark when designing a better neural network.

## 9. ACKNOWLEDGMENTS

This work is supported by the *Natural Sciences and Engineering Research Council of Canada (NSERC)*. The Mt. Bélair data were obtained from Hydro-Québec, and the authors thank Yvon Côté for his maintenance of the instrumentation in the difficult icing conditions of Mt. Bélair.

## 10. REFERENCES

Amat, J.L., Yahiaoui G., 1995, "Techniques avancées pour le traitement de l'information; Réseaux de neurones, logique floue algorithmes génétiques" CEPADUES-ÉDITIONS,

Chen T., Chen H., 1993, "Approximations of Continuous Functionals by Neural Networks with



Application to Dynamic Systems" IEEE Trans. Neural Networks, Vol 4, No 6, pp. 910-918

Hines, W.W., Montgomery, D.C., 1980. "Probability and Statistics in Engineering and Management Science" 2nd ed. John Wiley, New-York, 634 p.

Hornick, K., Stinchcombe, M., White, H., 1989, "Multilayer Feedforward Networks are Universal Approximators" Neural Networks, Vol 2, pp. 359-366.

McComber, P., Druetz, J., Laflamme, J., 1993, "Icing Rate Estimation of Atmospheric Cable Icing" Int. J. Offshore and Polar Eng., Vol 5 No 1, pp. 43-50

McComber, P., Druetz, J., Laflamme, J., 1995, "Icing Rate Estimation of Atmospheric Cable Icing" Int. J. Offshore & Polar Eng. Vol. 5, No. 2, pp. 75-92.

McComber, P., de Lafontaine, J., Laflamme, J. Druetz, J., Paradis, A., 1998 "A Neural Network

System to Estimate Transmission Line Icing" Proceedings 8<sup>th</sup> Int. Workshop on Atm. Icing of Structures, Reykjavik, Iceland, pp. 101-106.

Nordgren, R., Meckl P.H., 1993, "An Analytical Comparison of a Neural Network and a Model-based Adaptive Controller" IEEE Trans Neural Networks, Vol 4, No 4, pp. 685-694.

Ohta, H., Saitoh, K., Kanemaru, K., Ijichi, Y., Kitagawa, H., Konno, T., 1996, "Application of Disaster Warning System due to Snow Accretion on Power Lines Using Neural Networks" Proc. 7th IWAIS, Chicoutimi, pp. 149-154

Poots G., 1996, "Ice and Snow Accretion on Structures", John Wiley and Sons, 338 pp.

Wakamatsu, K., Yamamoto, Y., Kanemaru, K., Ijichi, Y., Kitagawa, H., Kanoh, H., Konno, T., 1993, "Development of Disaster Warning System due to Snow Accretion on Power Lines Using Neural Networks" Proc. 6th IWAIS, Budapest, pp. 175-180

